

Uncertainty in Climate Science: Not Cause for Inaction¹

Juan M. Restrepo,

Computer Science and Mathematics Division, Oak Ridge National Laboratory,
Oak Ridge TN, USA 37831

Michael E. Mann,

Department of Meteorology & Atmospheric Science, and The Earth and Environmental
Systems Institute, The Pennsylvania State University University Park, PA 16802

The Fourth National Assessment, Climate Science Special Report of the US Global Change Program, published in November 2017, concludes, "based on extensive evidence, that it is extremely likely that human activities, especially emissions of greenhouse gases, are the dominant cause of the observed warming since the mid-20th century."

When asked about some of the conclusions in the report regarding systematic climate change, Mr. Raj Shah, a spokesman for the Trump administration, stated, "The climate has changed and it is always changing. " Shah is echoing assertions from other observers that there is nothing unusual about the changes in climate and weather that we are experiencing: There have been changes before the industrial era, and some of these have been extreme. Translated to more technical terms, such observers claim that climate has a stationary statistical distribution –one that does not change with time– and that, in recent years, we just happen to be experiencing samples of this distribution that are, possibly rare, extreme highs. Shah continues, "[As the report] states, the magnitude of future climate change depends significantly on remaining uncertainty in the sensitivity of Earth's climate to greenhouse gas emissions" [21]. This part is hard to interpret, but it is meant to imply that climate forecasting is made unreliable by the presence of uncertainties. Shah's statement is fully consistent with the US Environmental Protection

¹This article appeared in print in two parts (without the material in the appendix of the present article), covering separately the two themes of this article: J.M. Restrepo, M. Mann, *This is how Climate is Always Changing*, SIAM News May 2018, and J.M. Restrepo, M. Mann, *This is how Climate is Always Changing*, Focus Group on Climate Newsletter, American Physical Society, March 2018. For citation purposes please use both of these articles. If a technical aspect presented in the appendix of this paper are required, please add a citation to this article as well.

Agency's (EPA) Pruitt's statements, such as "I think that measuring with precision human activity on the climate is something very challenging to do and there's tremendous disagreement about the degree of impact," he told CNBC. "So no, I would not agree that it's a primary contributor to the global warming that we see," Pruitt said. "But we don't know that yet, we need to continue to debate, continue the review and analysis" [5]. Acknowledging that climate changes but that the anthropogenic contribution is, *at the same time*, too difficult to estimate and too small to be of importance, is a frequently-used assertion of the Trump administration. Rather than disentangling the statement, we will instead address separately the issue of statistical stationarity of climate time series, and how climate predictions are impacted by uncertainties in natural and anthropogenic forcings.

To explore the assertion of a static climate distribution, we introduce here a theorem that applies to record values of a series of random variables drawn from a stationary distribution, such as the measured temperatures. Others have used this approach more rigorously to examine trends in climate data [2, 9, 23]. Since the only requirement made in the theorem on the random variables is that they derive from a stationary distribution, the failure of this theorem to hold indicates that the distribution from which this data arises is not stationary. The theorem or its application does not yield causal attributions to its outcomes. Nevertheless, the use of such a simple test circumvents the necessity to argue about data statistics based upon model outcomes.

We will also examine how the inclusion of historically-informed uncertainties on natural and anthropogenic greenhouse gases (GHG) modify climate predictions. To do this we will use a simple model that captures the essential phenomenology of the radiation balance of more complete state-of-the-art climate models. This *energy balance model* (EBM) will be used in what follows to determine whether uncertainties in GHG emissions lead to qualitatively different climate projections than those obtained without taking uncertainties into account.

Before proceeding we should clarify what is meant by climate, as opposed to weather. Climate and weather describe the same system, but the term 'climate' refers to large

spatio-temporal scales and 'weather' to small ones. This distinction is not just a convenience. While both describe the energetics, mass and momentum exchanges of a rotating Earth, the scale determines the prominence of the different phenomenology, weather being dominated by inertial effects (advective processes, turbulence, waves, density dynamics, and transient and sometimes unstable conditions) and climate by the forced/dissipative effects (radiation and ocean and atmospheric transport). Weather includes tornados, hurricanes, or extreme values of temperature or rainfall. Examples of climate are the seasons, El Niño/Southern Oscillation, the ice ages and Industrial Era global warming.

Records in Time Series

We make the following assertion: climate temperatures are samples from a stationary distribution. If so, a theorem that applies to stationary distributions should be borne out by the data. We apply a theorem about record highs and record lows (see [7]).

One draws a sequence of independent and identically-distributed (IID) samples X_1, X_2, \dots from a stationary distribution. We denote a sample from the sequence a *record* high (low) if its value is higher (or lower) than the samples preceding it. The probability of a record high is $P_n := \text{Prob}[X_n > \max\{X_1, X_2, \dots, X_{(n-1)}\}]$ (with the obvious modifications for the record low). In a sample set of size n any one particular value has equal chance of being the greatest (lowest) value, thus $P_n = 1/n$. We denote as $\mathbb{E}(R)$ the expected number of records for a stationary random sequence of size n . It is given by the harmonic series $\mathbb{E}(R) = 1 + 1/2 + 1/3 + \dots + 1/n$. For large n , $\mathbb{E}(R) = \gamma + \log(n)$, where γ is the Euler constant.

The occurrence of record values in climate data has been carefully compared to predictions for a stationary distribution (see, for example, [2], [9], [23]). Just to convey a feeling for such analyses, we undertake here a much less rigorous but hopefully illuminating look at some data. It should be cautioned that the application of this theorem

to real data is highly nontrivial. Hence, in what follows, we will be using this exercise merely to give a suggestive outcome.

If the theorem applies to climate data, we expect to wait increasingly long times for each new record temperature value (either high or low) because the probability declines as $1/(t - t_0)$, where the time t of each temperature observation takes the place of the statistical index n , and t_0 is the start of the particular temperature observations. (If the probability distribution were symmetric we would also expect the rates of record highs and lows to be similar).

Figure 1a compares the record high/lows obtained from a synthetic random time series to the July temperatures measured at the Moscow station, from about 1880 to 2011 [16]. For the random time series, the highs and lows are similarly spaced in time. However, for the Moscow temperature data, one sees many lows occurring at the early times and none after about 1910. By contrast, the record highs are more spaced out in time and continue through the observation period shown. The data suggests that the theorem on records is not fulfilled and that the rate at which record highs or lows occur at time t does not follow $1/(t - t_0)$.

Figures 1b and c plot temperature data (from [16]) from 30 locations in the Northern Hemisphere. The locations were chosen at random but were mostly concentrated around temperate zones, simply because these records tended to be longer. The time series are not all the same length and some stations did not report every year. The superposition of the data in Figure 1b would lead you to believe that, over the course of the industrial revolution, a stationary distribution of temperatures is not all that bad a statistical model. In that figure we highlight seven temperature time series, chosen arbitrarily. The records associated with these 7 data are plotted in Figure 1c. To facilitate comparison, these seven data sets have been adjusted by subtracting the first temperature in the set (thus the adjusted temperature of any of these time series was 0). Adding more observations to the top set or more observations to the bottom set does not change the impression that, with time, more high records will occur than low records (the low records stop occurring). The key observation is that the record highs and the record lows do not

obey the $1/t$ dependence. Another test would be to compute the expectation of the number of records to see if it is logarithmic, but doing so requires either longer data sets or a larger collection of data sets, such as the combined readings of all stations in the US.

The key observation is that the record highs and the record lows do not obey the $1/t$ dependence. Hence, these temperature records must not samples from a stationary process.

Wergen and Krug [25], [24], [9] and others, have taken this line of research much further, to include correlations, a multiplicity of distributions, consideration of spatial dependence. They have also found that removing a trend in the data makes the theorem more likely to be consistent with the statistics of temperature data. The values obtained for the trend, using this analysis, are consistent with estimates of a rate of increase in the global mean temperature of about 0.7°C in the land/ocean temperature over the last century, roughly ten times faster than the average rate of ice-age-recovery warming (see NOAA web site. Also see <https://globalclimate.ucr.edu/resources.html> for educational material on this topic).

In summary, the data suggests that Earth's climate is a non-stationary process. This is something climate scientists would find consistent with what we know about climate. Hence, it is not likely that the temperature extremes that we experience today are rare events, but rather, the result of a changing climate. The findings of this line of inquiry, using much more technical assumptions and allowing for correlations and for a multiplicity of probability distributions, indicates that climate has been severely biased upward during the Industrial Era. The use of this theorem to estimate the return time of record high temperatures would seriously underestimate the occurrence of historical highs, and overestimate historical lows.

Incorporating Uncertainties in Greenhouse Gas (GHG) Projections

Global estimates of GHG emissions are readily available (see [3]) and their estimates have tightly constrained uncertainties, since these are critical to the economy of the energy sector. Private and public entities keep track of production and resources fairly accurately. Uncertainties are associated, however, with how to regulate and tax GHG. This uncertainty is financially significant, but these would affect the design of commodity trading treaties, just as uncertainties in many other commodities routinely affect how they are traded. Uncertainties in the effect of GHG on climate play out locally: there are well-recognized uncertainties related to transport and dispersion as well as to critical dependencies on their interaction with their environment (land, oceans, atmosphere). However, we are going to focus here on variability spanning several decades to hundreds of years and the largest of spatial scales. At these scales local nuances are not resolved and a balance model yields the temporal evolution of a global temperature T .

By incorporating uncertainties into the temperature and radiative forcings we can explore to what extent uncertainties in GHG affect conclusions of future projections of the temperature. The uncertainties are derived from a statistical analysis of the historical data. We can compare natural and anthropogenic GHG forcings, taking into account uncertainties, in order to determine whether the sensitivity of the outcomes depends on the relative uncertainties in these two GHG components. We can also infer whether natural or anthropogenic forcings are dominant, prior to the Industrial Era, during this Era, and in the future.

Black body radiation tells us that the earth's radiation is proportional to T^4 . The surface energy balance, in terms of the surface temperature T , is $CdT/dt = Q + \kappa\sigma T_{Atm}^4 - \sigma T^4$, where T_{Atm} is the atmospheric temperature, t is time, C is the effective heat capacity, and σ is Stefan-Boltzmann constant. Q is the effective incoming radiation. If $C_a dT_{Atm}/dt$ is small, where C_a is the atmospheric effective heat capacity, then $\kappa\sigma T^4 + 2\kappa\sigma T_{Atm}^4 \approx 0$, then $CdT/dt = Q - (1 - \frac{\kappa}{2})\sigma T^4$. The range of temperatures of the

process is not large, hence, $(1 - \frac{\kappa}{2})\sigma T^4 = A + BT$, is a linearization and the constants in the nonlinear formula are subsumed by A and B . The energy balance is spectrally dependent: the high frequency component has a portion that reflects back to space by clouds and snow/ice and one that mostly dissipates. The low frequency component, on the other hand, is affected by reflectivity and the presence of a complex layer of gas, dust, and droplets which is capable of trapping the surface outgoing radiation. Q will be assumed to be a linear combination of the effective solar radiation and the radiative forcing due to GHG. Hence $Q = \frac{1}{4}(1 - \alpha)S + F_{GHG}$, where the albedo $\alpha \approx 0.3$, and the global average solar radiation $S/4 \approx 1370/4 \text{ Wm}^{-2}$, presently. (See [14], [17], and [12]). The Energy Balance Model (EBM) we adopt is thus

$$CdT = \frac{S}{4}(1 - \alpha)dt + F_{GHG}dt - (A + BT)dt + \nu(t), \quad (1)$$

where T is the temperature of Earth's surface (approximated as the surface of a 70-meter-depth, mixed-layer ocean covering 70 percent of Earth's surface area). $C = 2.08 \times 10^8 \text{ J K}^{-1}\text{m}^{-2}$ is the effective heat capacity that accounts for the thermal inertia of the mixed-layer ocean, but does not allow for heat exchange with the deep ocean as in more elaborate 'upwelling-diffusion models' ([26]). The last term in the equation is a stochastic forcing term, added to represent inherent uncertainties and unresolved processes (Hasselmann, [8], spearheaded the conceptualization of low dimensional models for climate with an unresolved physics that had its own, possibly stochastic, dynamic). The model (1) appears in [10] (and a link is provided to matlab code which can be used to reproduce the temperature outcomes in that article). The choice $A = 221.3 \text{ Wm}^{-2}$ and $B = 1.25 \text{ WK}^{-1}\text{m}^{-2}$ yields a realistic preindustrial global mean temperature $T = 14.8^\circ\text{C}$ and an equilibrium climate sensitivity (ECS) of $3.0 \text{ }^\circ\text{K}$, consistent with midrange estimates by the International Panel on Climate Change ([22]), as the range is likely somewhere between $1.5 - 4.5$. The equilibrium climate sensitivity is defined as the temperature change due to the effect of doubling in the concentration of CO_2 in Earth's atmosphere. A 1°K change requires a doubling of CO_2 , or equivalently, to an increased forcing of 3.7 W m^{-2} .

The model was driven with estimated annual natural and anthropogenic forcing over the years A.D. 850 to 2012. Greenhouse radiative forcing was calculated using the

approximation $F_{GHG} = 5.35 \log(\text{CO}_{2e}/280)$, where 280 parts per million (ppm) is the pre-industrial CO_2 level and CO_{2e} is the 'equivalent' anthropogenic CO_2 (see [15]). The CO_2 data from Ammann *et al* [1] is used, scaled to give CO_{2e} values 20% larger than CO_2 alone (for example, in 2009 CO_2 was 380 ppm whereas CO_{2e} was estimated at 455 ppm). Northern Hemisphere anthropogenic tropospheric aerosol forcing was taken instead from Crowley [6], with an increase in amplitude of 5% to accommodate for a slightly larger indirect effect than in [1]. A linear extrapolation of the original series (which ends in 1999) is used to extend through 2012². In the simulations we have assumed that tropospheric aerosols decrease exponentially from their current values with a time constant of 60 years. This gives a net anthropogenic forcing change from 2000 to 2100 of 3.5 Wm^{-2} , roughly equivalent to the International Panel on Climate Change's 5th assessment report 'RCP6' scenario, a future emissions scenario that assumes only modest efforts at mitigation. Estimated past changes in solar irradiance were prescribed as a change in the solar constant S whereas forcing by volcanic aerosols was prescribed as a change in the surface albedo α . Solar and volcanic forcing were taken from the General Circulation Model (GCM) simulations described in McGuffie and Henderson-Sellers [14]. These were modified as follows: the solar forcing was rescaled under the assumption of a 0.1 percent change from Maunder Minimum to present, more consistent with recent estimates ([1]); the volcanic forcing applied was the mean of the latitudinally varying volcanic forcing in Ammann *et al* [1]. With no added uncertainties, solar output and no climatically-significant volcanic eruptions were assumed, for the years 2012-2100. CO_2 radiative forcing has been extrapolated linearly, till the year 2100, based on the trend over the past decade (which is roughly equivalent, from a radiative forcing standpoint, to a forward projection of the exponential historical trajectory of CO_2 emissions). A net tropospheric anthropogenic aerosol forcing rate decrease of 0.7 Wm^{-2} per year, starting with the year 2000 has been taken into account in the model.

²One needs to distinguish between emissions and CO_2 concentrations. The latter are directly measurable in the atmosphere and the increase is monotonic. This forms the basis for the extrapolation model.

As summarized in the IPCC report the net rise in temperature during the Industrial Era is due to the upward trend of the anthropogenic GHG forcing. What's more, there is no way to predict the temperature increases measured during the Industrial Era, solely, by natural forcing. Figure 2 depicts EBM temperature predictions as a function of various values of the equivalent climate sensitivity (ECS) with historically-based additive uncertainties added. Variations on ECS convey the sensitivity of the predictions to epistemic uncertainties in the models. The instrumental record appears in black in the figure. The temperature predictions shown represent single realizations of the energy balance model. Details of the temperature noise model appear in the Appendix. The outcome suggests that taking into account historically-informed temperature variability in the predictions does not alter the conclusion that the upward trend in the anthropogenic forcing remains dominant factor in explaining temperature rises during the Industrial Era. We examine next whether taking into account stochastic variability in the natural as well as anthropogenic forcing changes this conclusion. Figure 3 portrays temperature predictions from EBM model runs that incorporate uncertainties in the natural forcing. In Figure 3a we include, exclusively, volcanic forcing uncertainties. In Figure 3b we allow for solar forcing uncertainties. The various curves result from using different ECS values. The description of the uncertainty models for volcanic, solar, and CO₂ source variability is found in the Appendix. Plotting a single realization, it is hoped, conveys qualitatively the relative impact of the stochasticity on the outcomes (qualitative characteristics of the sample moments can be easily inferred from the specific noise models used). As is expected, the temperature reacts abruptly to highly localized volcanic emissions and the sensitivity to solar variability is small, comparatively. Hence, a significantly larger portion of the variance in an ensemble of these predictions is attributed to the volcanic emissions, rather than the solar uncertainties.

Figure 4 shows the stochastic long wave and short wave forcing contributions over time. The composite indicates a dominant role for the long wave component during the last 50 years: the trend is larger than its inherent variability. In Figure 5 we depict a single realization of the temperature predictions, driven by the forcing described in Figure 4, *i.e.*, the temperature predictions taking into account natural and anthropogenic forcing and their variability. The upward trend in the long-wave emissivity still dominates over

any uncertainties due to natural *and* anthropogenic forcings during the Industrial Era. In the end the steady-increasing CO₂ forcing is overwhelming the temperature predictions in the Industrial Era and into the future, even when taking into account the variability due to volcanic and solar forcing.

Summary

Without making use of anything more than data we have shown that temperatures around the Northern Hemisphere do not have a time-stationary distribution. More careful analysis of the data has shown that this is a general statement regarding temperature most anywhere on Earth. Fits of the data, for Industrial Era temperatures, show an upward trend. Ocean temperature surveys also indicate that the temperature of the ocean in the upper 2000m has increased. The signal-to-noise ratio of this Argo data, collected for the last 20 years, is much higher than near-ground atmospheric temperatures [4]. In fact, data and models indicate that the global mean temperature of the Earth is increasing, since the end of the 19th century [18]. With a changing climate, we have observed a changing weather. The rate at which climate is changing is alarming since it is comparable to, or shorter than, the typical relaxation rates of the system (land, ocean, and atmosphere).

An energy balance model, consistent with instrumental data, was used here to explore how the inclusion of inherent uncertainties affect the relative impact of natural and anthropogenic forcing on Earth's temperature [10]. We estimated uncertainties from the data and constructed historically-informed models for the variability of each of the forcings. Both of these forcings need to be invoked to get the model to agree with data. Driven by estimated natural and anthropogenic radiative forcing, our calculations indicate that the warming is a result of anthropogenic increases in greenhouse gas concentrations and that the inclusion of aleatoric uncertainties do not change this outcome in the ensemble sense. Moreover, since the effect of forcing variability is small compared to the upward trend of the anthropogenic forcing, the inherent variability does not offer

much of a reason to expect that the temperature will keep climbing unless there is a rate slowdown in the anthropogenic forcing, *i.e.*, in the production of GHG. Using far more sophisticated models and state-of-the-art knowledge in climate, scientists reach the same conclusions [22] and further, have not been able to find a non-anthropogenic explanation to the observed increase in warm extremes in global temperatures during the Industrial Era (*e.g.*, [11]).

The key natural forcings are associated with volcanic emissions and changes in insolation. While statistical projections of changes in natural volcanic and solar radiative forcing of climate are by necessity speculative, we find no evidence that such natural radiative forcing changes could substantially alter the projected warming from increasing greenhouse gas concentrations. The impact of their variability would contribute to known unknowns in the temperature uncertainty. The long-time features of the model and the historical data agree well and thus do not require postulating or requiring epistemic variability (unknown unknowns).

Shah's appraisal of the outcomes in the Fourth National Assessment report offered us an invitation to demonstrate how simple, well established, quantitative methods are used to address apparent challenges posed by uncertainties in climate assessments. Given the evidence that key climate change attributes, such as ice sheet collapse and sea level rise, are occurring ahead of schedule [13] uncertainty has in many respects broken against us, rather than in our favor. Scientific uncertainty is not a reason for inaction. If anything, it is a reason for more concerted efforts to limit carbon emissions

Acknowledgements

We want to thank Barbara Levi who provided invaluable editorial assistance with this article.

References

- [1] C. M. AMMANN, F. JOOS, D. SCHIMEL, B. OTTO-BLIESNER, AND R. TOR-MAS, *Solar influence on climate during the past millennium: Results from transient simulations with the ncar climate system model*, Proceedings of the National Academy of Sciences, 104 (2007), pp. 3713–3718.
- [2] R. BENESTAD, *Record-values, nonstationarity tests and extreme value distributions*, Climate Research, 25 (2003), pp. 3–13.
- [3] T. BODEN, G. MARLAND, AND R. ANDRES, *Global, Regional, and National Fossil-Fuel CO₂ Emissions*, Carbon Dioxide Information Analysis Center, Oak Ridge National Laboratory, U.S. Department of Energy, 2017. doi:10.3334/CDIAC/00001_V2017.
- [4] L. CHENG, K. TRENBERTH, J. FASULLO, T. BOYER, J. ABRAHAM, AND J. ZHU, *Improved estimates of ocean heat content from 1960 to 2015*, Science Advances, 3 (2017), p. e1601545.
- [5] D. CHIACU AND V. VOLCOVICI, *EPA Chief Pruitt Refuses to Link CO₂ and Global Warming. Scott Pruitt cites a need to 'continue the review and analysis' despite strong push back from scientists*, Scientific American and Reuters, (2018).
- [6] T. CROWLEY, *Causes of climate change over the past 1,000 years*, Science, 289 (2000), pp. 270–277.
- [7] F. G. FOSTER AND A. STUART, *Distribution-free tests in time-series based on the breaking of records*, Journal of the Royal Statistical Society. Series B, 16 (1954), pp. 1–22.
- [8] K. HASSELMANN, *Stochastic climate models. part I.theory*, Tellus, 28 (1976), pp. 473–485.
- [9] J. KRUG, *Records in a changing world*, Journal of Statistical Physics, (2007), p. P07001. doi:10.1088/1742-5468/2007/07/P07001.

- [10] M. MANN, *Why global warming will cross a dangerous threshold in 2036*, Scientific American, (April 1, 2014).
- [11] M. MANN, S. MILLER, S. RAHMSTORF, B. STEINMAN, AND M. TINGLEY, *Record temperature streak bears anthropogenic fingerprint*, Geophysics Research Letters, 44 (2017). doi:10.1002/2017GL074056.
- [12] M. MANN, B. STEINMAN, AND S. K. MILLER, *On forced temperature changes, internal variability and the AMO*, Geophysics Research Letters, 41 (2014), pp. 3211–3219.
- [13] M. MANN AND T. TOLES, *The Madhouse Effect: How Climate Change Denial Is Threatening Our Planet, Destroying Our Politics, and Driving Us Crazy*, Columbia University Press, 2016.
- [14] K. MCGUFFIE AND A. HENDERSON-SELLERS, *A Climate Modeling Primer*, Wiley, 2 ed., 1997.
- [15] G. MYHRE, E. HIGHWOOD, K. SHINE, AND F. STORDAL, *New estimates of radiative forcing due to well mixed greenhouse gases*, Geophysics Research Letters, 25 (1998), pp. 2715–2718.
- [16] NASA/GISS, *Surface temperature analysis*. data.giss.nasa.gov/gistemp/, 2013.
- [17] G. R. NORTH, R. CAHALAN, AND J. COAKLEY, *Energy balance climate models*, Reviews of Geophysics, 19 (1981), p. 91?121.
- [18] R. PACHAURI AND L. MEYER, eds., *IPCC, 2014: Climate Change 2014: Synthesis Report. Contribution of Working Groups I, II and III to the Fifth Assessment Report of the Intergovernmental Panel on Climate Change, [Core Writing Team]*, IPCC, 2014.
- [19] J. RESTREPO, S. VENKATARAMANI, D. COMEAU, AND H. FLASCHKA, *Defining a trend for a time series using the intrinsic time-scale decomposition*, New Journal of Physics, 16 (2014), p. 085004. doi:10.1088/1367-2630/16/8/0850004.

- [20] J. M. RESTREPO AND S. VENKATARAMANI, *Stochastic longshore current dynamics*, *Advances in Water Resources*, 98 (2016), pp. 186–197.
- [21] R. SHOWSTACK, *Experts ponder why administration released tough climate report*, *Eos*, 98 (6 November, 2017). doi:10.1029/2017EO086297.
- [22] S. SOLOMON, D. QIN, M. MANNING, Z. CHEN, M. MARQUIS, K. B. AVERYT, M. TIGNOR, AND H. L. MILLER, *IPCC, 2007: Climate Change 2007: The Physical Science Basis*, Cambridge University Press, Cambridge, 2007. Contribution of Working Group I to the Fourth Assessment Report of the Intergovernmental Panel on Climate Change.
- [23] G. WERGEN, *Records in stochastic processes: theory and applications*, *Journal of Physics, A: Mathematics, Theory*, 46 (2013), p. 223001. doi:10.1088/1751-8113/46/22/223001.
- [24] G. WERGEN, J. FRANKE, AND J. KRUG, *Correlations between record events in sequences of random variables with a linear trend*, *Journal of Statistical Physics*, 144 (2011), pp. 1206–1222.
- [25] G. WERGEN AND J. KRUG, *Record-breaking temperatures reveal a warming climate*, *European Physics Letters*, 92 (2010), p. 30008. doi:10.1209/0295-5075/92/30008.
- [26] T. WIGLEY AND S. RAPER, *Natural variability of the climate system and detection of the greenhouse effect*, *Nature*, 344 (1990), p. 324–327.

Appendix, Stochastic Parameterizations

We describe the parametrization of the natural and anthropogenic forcing, used in the future projections produced with the EBM model, (1). The process for the stochastic parametrization follows the strategy used in [20].

Volcanic Emissions: Using historical data from [1], we propose the following stochastic model:

$$dy(t) = -by(t)dt + \exp(\mathcal{J}_t)dP_t,$$

where $b = 260/365$, \mathcal{J}_t is an exponential process with uniform random argument $1.2\mathcal{U}[0, 1]$, and dP_t is a Poisson incremental process with $\lambda = 0.07$. Figure 6 shows a comparison of the data (lower), and the negative of the stochastic simulation (upper).

Solar Forcing: The solar data for the years 850-2012 AD from [1] is used. In what follows, the mean 1365.8 W/m^2 is removed. Figure 7a displays the modulus of the spectral decomposition of the (periodized) observations. Figure 7b features the observations and the parametrization, along with the intrinsic time decomposition of the signal [19]. The intrinsic time decomposition of the signal $s(t) = b(t) + r(t)$, is not lossy. The baseline $b(t)$ is designed to lace through the data in such a way that local maximas (minimas) of the time series $s(t)$ are below (above) the baseline at the locations of the extremas. At the extremal locations the baseline is situated at the three-point average of the extreme and its two neighbors. The rest of the baseline is constructed by linear interpolation. The rotation signal is defined by $r(t) = s(t) - b(t)$. The parametrization $\sigma(t) = b(t) + n(t)$, where $n(t)$ is an ARMA(4,0) process obtained from the rotation $r(t)$. In the ARMA, the constant was -0.0010598 , $p_1 = 1.7193$, $p_2 = -1.192$, $p_3 = 1.0518$, $p_4 = -0.58531$. The standard error on these was less than one percent. The extrapolation of $\sigma(t)$ beyond the observations, *i.e.*, beyond 2012, is obtained by a reset of time in $b(t - t_r)$, where t_r is drawn at random from the years 928 and 1924. The value of the solar observations at 2012 is used to adjust the extrapolation. The baseline assumed free boundary conditions at the ends of the observation record. The time scales in the ARMA process was large enough that, for short extrapolations of the signal, in the interval 2012-2100, it was impossible to discern the persistence of the baseline signal. Figure 7c depicts the signal plus its extrapolation beyond year 2012.

CO₂ Forcing Rate: We use a deterministic fit $\kappa_i(t)$, obtained by least squares, from the CO₂ forcing signal. There are two fitted regions, namely,

$$\kappa_1(t) = \sum_{i=0}^4 a_i \tilde{y}^i,$$

where \tilde{y} = year-1770, with parameters $a_4 = -1.59 \times 10^{-7}$, $a_3 = 5.93 \times 10^{-5}$, $a_2 = -0.006$, $a_1 = 0.265$ and $a_0 = 278$, for the years 1770 – 1955, and

$$\kappa_2(t) = \sum_{i=0}^2 a_i \tilde{y}^i,$$

where \tilde{y} = year-1956, for the span 1956 – 2012, with parameters $a_2 = 0.012$, $a_1 = 0.7943$, and $a_0 = 394.7128$. We combine the variability $T(t) - \kappa_1(t)$ of 1770 – 1955, and $T(t) - \kappa_1(t)$ of 1956 – 2012, and propose an AR(1) model (constant = -0.077584 and $p_1 = 0.80513$), with variance 0.17 yr^2 . We then use $\kappa_2(t)$ to extrapolate to the year 2100 AD, adding the AR(1) process for variability. See Figure 8.

Parametrizing Future Temperature Uncertainty:

The temperature uncertainty $\nu(t)$ is parametrized as follows. We use compilations of the Northern Hemisphere temperatures, for the years 1850-2012 AD (see [10]). An ARIMA analysis of the raw data was performed, double differencing the data. The outcomes were satisfactory, but not as robust as using a fitted removal of the trend and a noise model for the residual. The parametrization consists of a trend τ plus a stochastic parametrization of $T - \tau$, where T is the normalized temperature record. The fit of the trend is

$$\tau = \sum_{i=0}^3 a_i \tilde{y}^i$$

where \tilde{y} =year-1850, and $a_3 = 2.644 \times 10^{-7}$, $a_2 = -7.98 \times 10^{-6}$, $a_1 = -0.000167$, $a_0 = -0.274$. The residual $T - \tau$ is represented well (according to the Bayesian Index Criteria, BIC), by an AR(1), with constant = -3.0333×10^{-5} , $p_1 = 0.53426$, with errors in the order of 6 percent.

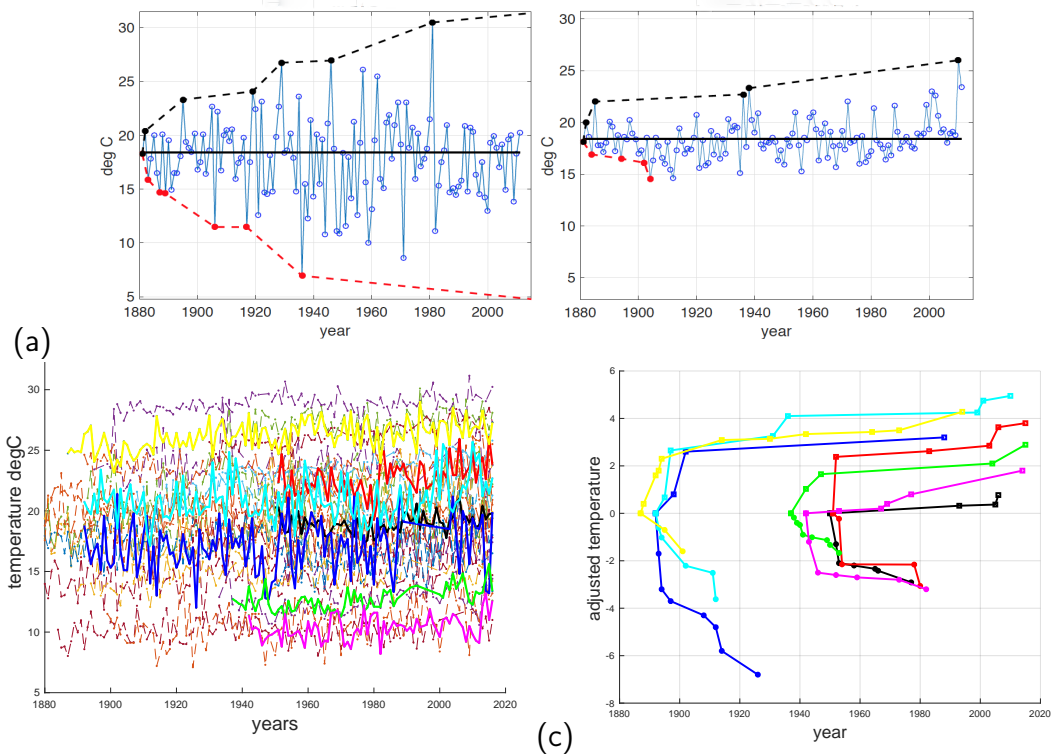


Figure 1: (a) (left) records in a synthetic stationary distribution, (right) records of July monthly temperatures at the Moscow station; (b) temperature data, as a function of time, for 30, arbitrary locations in the Northern Hemisphere; (c) Record values for seven temperature time series, highlighted in (b). The adjusted temperature subtracts out the first temperature value in the time series. The data is taken from GISS repository. We note that you reach a time in each data set beyond which no new lows occur whereas new highs continue to appear going forward in time. Temperature in degrees $^{\circ}\text{C}$.

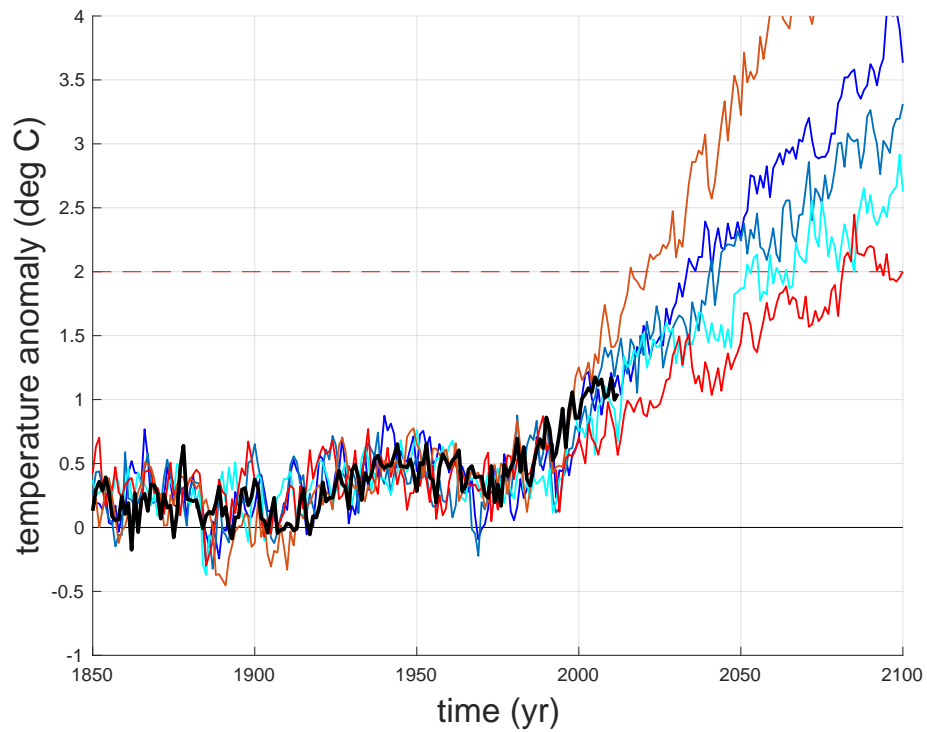
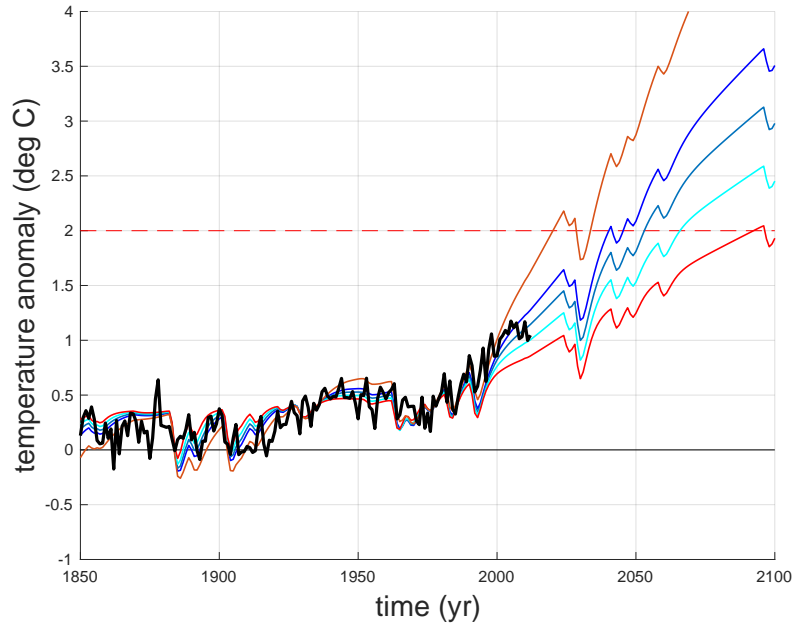
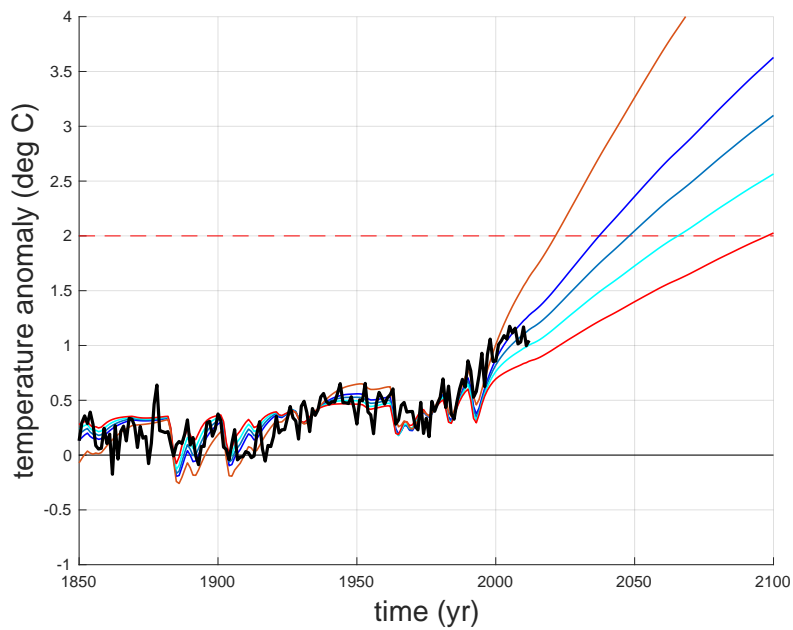


Figure 2: Temperature prediction, as a function of time, for various values of equivalent climate sensitivity (ECS). Shown, a single realization for each ECS. The stochastic model for the temperature was informed by instrumental data. From top to bottom, $ECS = 4.5, 3, 2.5, 2, 1.5$. The instrumental record appears in black.



(a)



(b)

Figure 3: Temperature predictions, as a function of time for various equivalent ECS values. A single realization is depicted, and the same stochastic model outcome is used in each of the ECS cases. In (a) predictions are made by accounting, exclusively, for stochastic volcanic forcing variability. In (b) for stochastic solar forcing variability exclusively. From top to bottom, $ECS = 4.5, 3, 2.5, 2, 1.5$. The instrumental record is depicted in black.

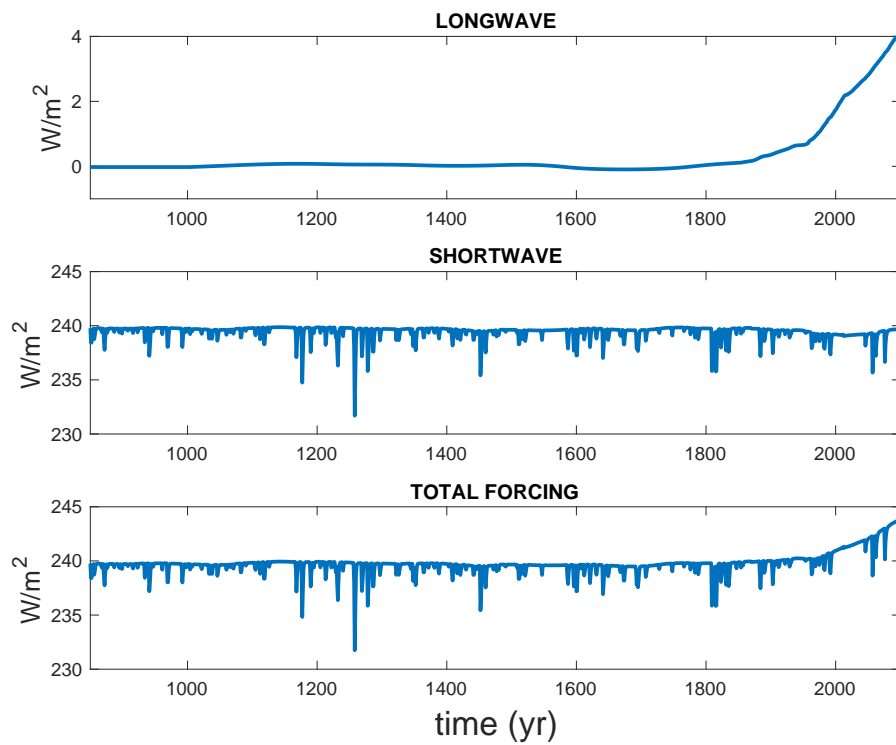
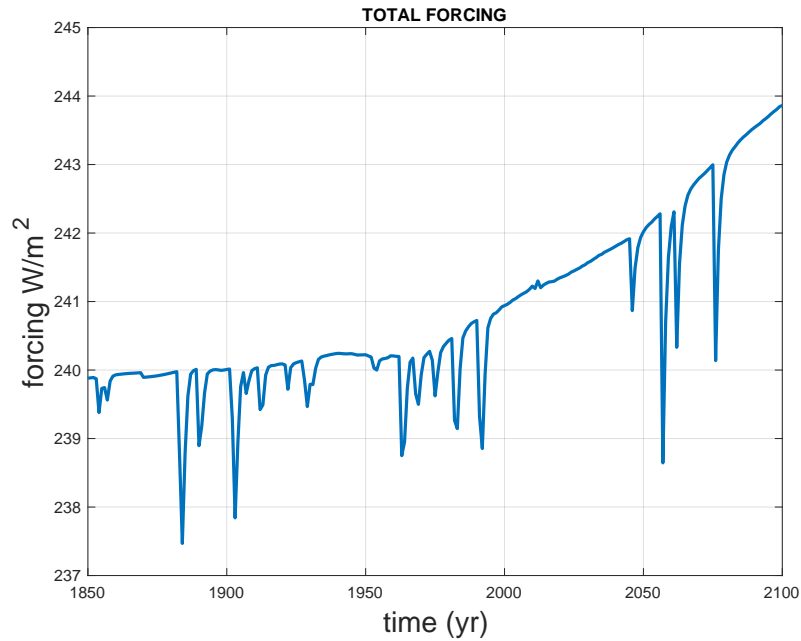
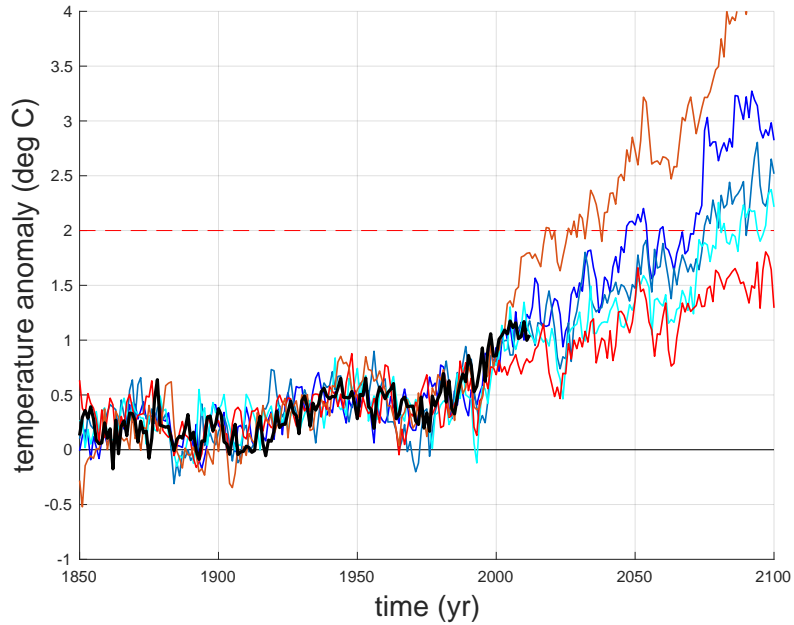


Figure 4: Stochastic long wave, short wave forcing and composite total forcing, with uncertainties due to CO₂ emissions, volcanic activity, and solar forcing. A single stochastic realization is depicted.



(a)



(b)

Figure 5: (a) Highlight of the composite forcing appearing in Figure 4 corresponding to the period 1850-2100; (b) temperature predictions as a function of ECS, taking into account uncertainties due to CO₂ emissions, volcanic activity, solar forcing. Stochastic variability due to temperature uncertainties has been included. The stochastic model for temperature fluctuations is informed by historical temperature variability data. From top to bottom, $ECS = 4.5, 3, 2.5, 2, 1.5$

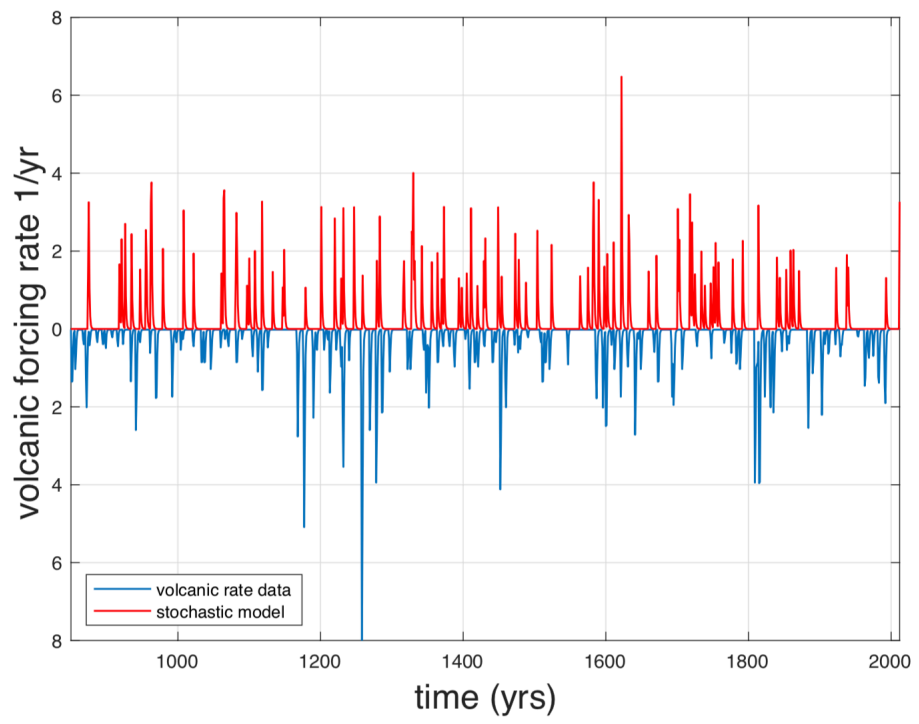


Figure 6: Lower: volcanic forcing data; upper, stochastic parametrization.

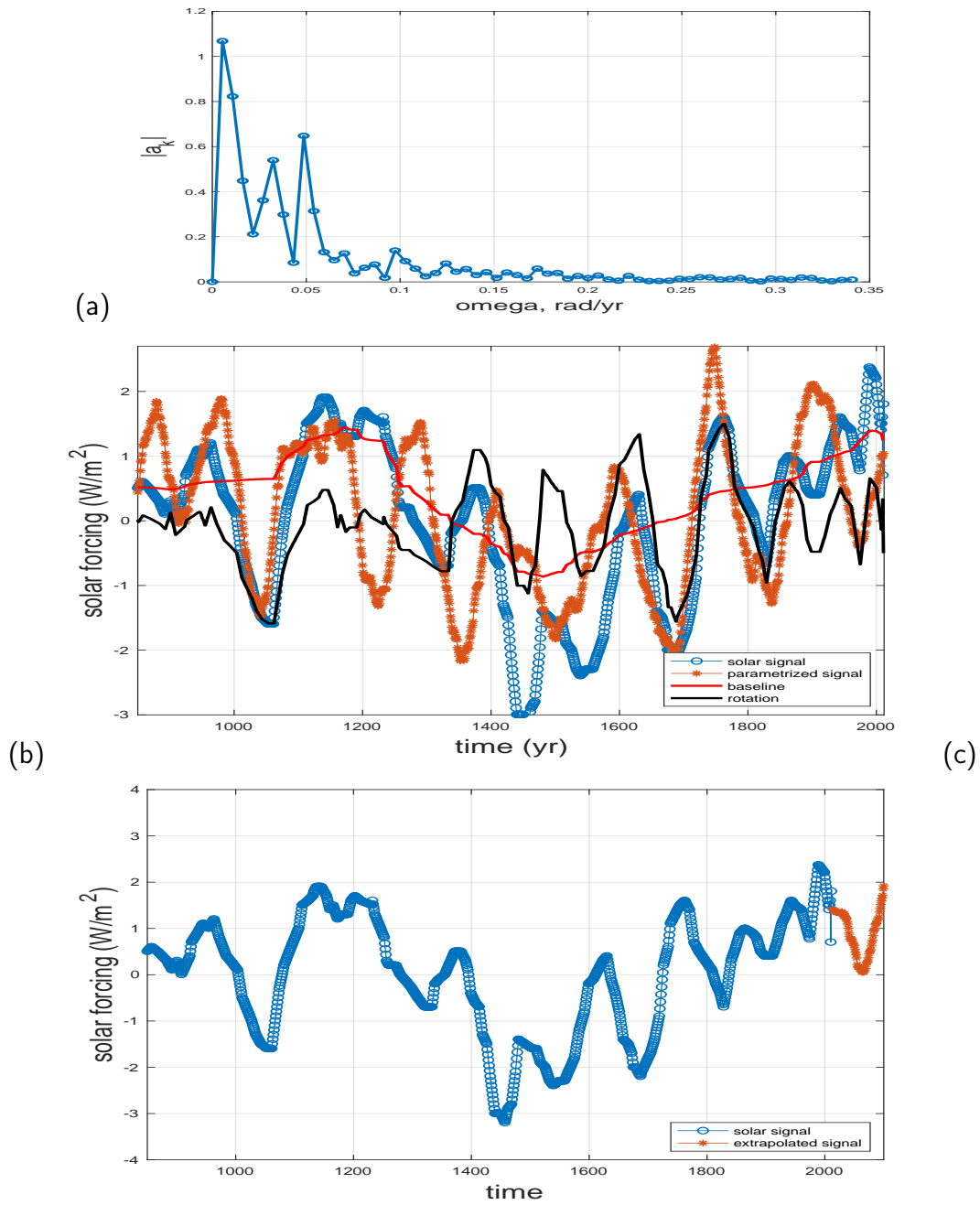


Figure 7: Solar forcing (W/m^2). The historical mean 1366 W/m^2 is subtracted. (a) Spectrum of the observations; (b) comparison of data and the parametrization of the solar forcing. Data (*), parametrization (o). The baseline (blue) and the rotation (red) from the intrinsic time decomposition; (c) observations (o) and extrapolated (*) solar forcing.

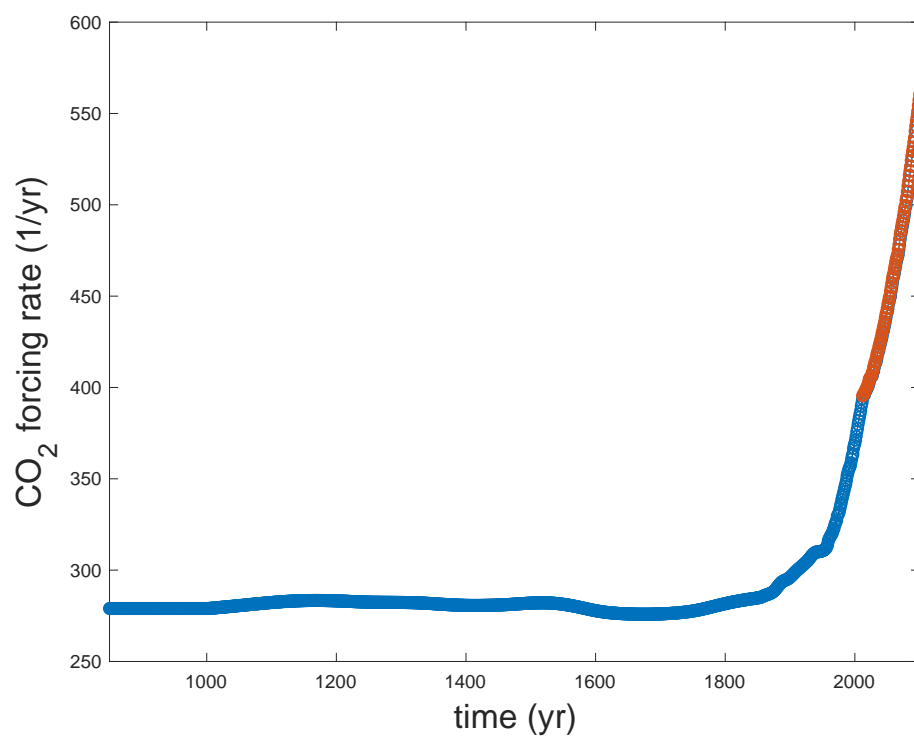
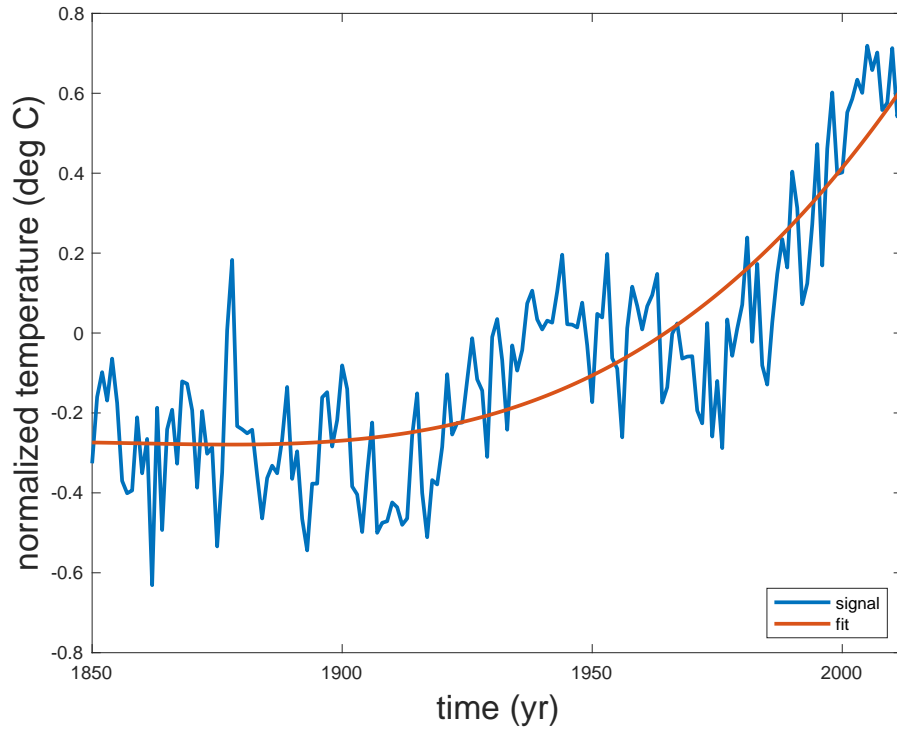
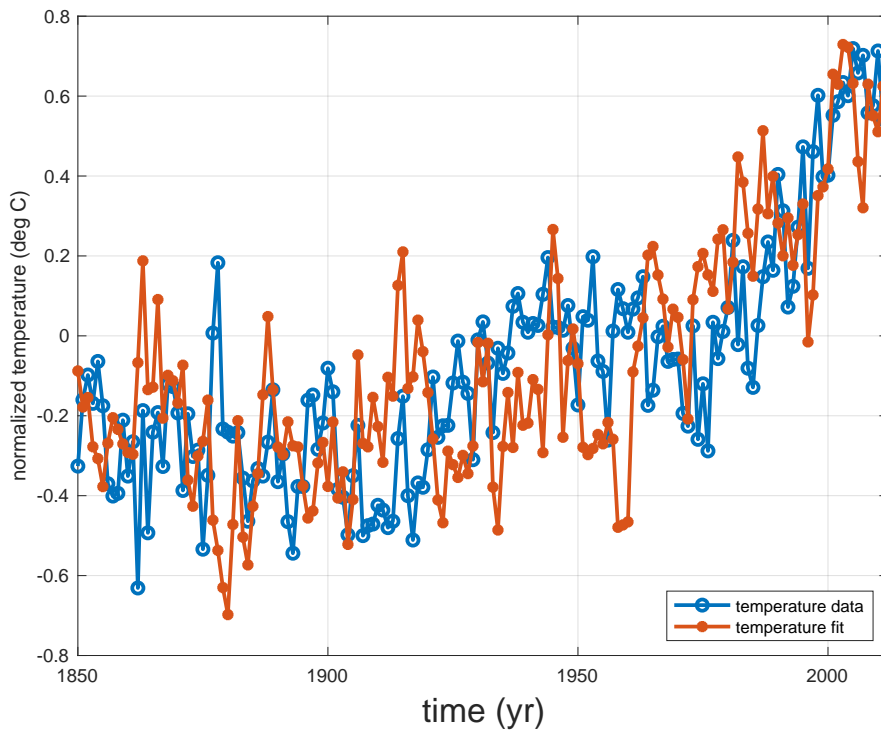


Figure 8: Superposition of the CO₂ forcing rate data and the stochastically-fitted version; in red, stochastic parametrization for the years 2012 – 2100.



(a)



(b)

Figure 9: (a) Fit of the trend $\tau = \sum_{i=0}^3 a_i \tilde{y}^i$, where $\tilde{y} = \text{year} - 1850$, and data to the temperature distribution; (b) stochastic parametrization and data.